Araştırma Makalesi
Adıyaman Üniversitesi
Mühendislik Bilimleri Dergisi
20 (2023) 141-155

DESIGN OF THE PERMANENT MAGNET SYNCHRONOUS MOTOR USED IN ELECTRIC VEHICLES WITH THE HELP OF THE PARTICLE SWARM ALGORITHM AND ANSYS-MAXWELL

Yıldırım ÖZÜPAK[1], Mehmet ÇINAR[2*]

[1]Silvan Vocational School, Electrical Department, Dicle University, Diyarbakır, 21000, Turkiye
[2]Tatvan Vocational School, Electrical Department, Bitlis Eren University, Bitlis, 13210, Turkiye
Geliş Tarihi/Received Date: 15.06.2023 Kabul Tarihi/Accepted Date: 06.09.2023 DOI: 10.54365/adyumbd.1315079

ABSTRACT

Performance and efficiency are among the most important parameters in electric motors. Improvements to the engine not only increase engine performance but also affect production costs. Permanent Magnet Synchronous Motor (PMSM) is a motor widely used in electric vehicles because of its high torque density, high efficiency, and production advantages. In this study, a 110 kW (Adjust-Speed Permanent Magnet Synchronous Motor) AS-PMSM was designed for electric vehicle applications. The results of the ANSYS-Maxwell and Particle Swarm Optimization (PSO) algorithm and the calculations of the optimized design were compared in line with the obtained data. In the design study, theoretical calculations, the PSO algorithm, and finite element method (FEM)-based ANSYS-Maxwell software were used. Based on these values, the computer-aided design of the engine was carried out. First of all, the basic design and performance criteria of the engine were determined. Parameters of the motor, such as torque ripple, iron loss, efficiency, and electromagnetic analysis, were analyzed and optimized with ANSYS-Maxwell. Then, electrical, magnetic, and performance analyses of the motor were made. How engine performance changes with the methods used has been examined in detail. Efficiency values were determined under various operating conditions in engine performance studies. The validity of the improvement study and the verification of the design study were examined by comparing the ANSYS results with the PSO algorithm results. The analysis results showed that the designed electric motor met the desired power values and design performance criteria.

Keywords: *PMSM, FEM, Design, Efficiency, PSO*

ELEKTRİKLİ ARAÇLARDA KULLANILAN KALICI MIKNATISLI SENKRON MOTORUN PARÇACIK SÜRÜ ALGORİTMASI VE ANSYS-MAXWELL YARDIMIYLA TASARIMI VE ANALİZİ

ÖZET

Elektrik motorlarında performans ve verimlilik en önemli parametreler arasındadır. Motor üzerinde yapılacak iyileştirmeler sadece motor performansını artırmakla kalmıyor, aynı zamanda üretim maliyetlerine de etki ediyor. Kalıcı Mıknatıslı Senkron Motor (KMSM), yüksek tork yoğunluğu, yüksek verim ve üretim avantajları ile elektrikli araçlarda yaygın olarak kullanılan bir motordur. Bu çalışmada, elektrikli araç uygulamaları için 110 kW (Adjust-Speed Kalıcı Mıknatıslı Senkron Motor) AS-KMSM tasarımı yapılmıştır. ANSYS-Maxwell ve Parçacık Sürü Optimizasyonu (PSO) algoritması sonuçları ve optimize edilen tasarımın hesaplamaları, elde edilen veriler doğrultusunda karşılaştırılmıştır. Tasarım çalışmasında teorik hesaplamalar, PSO algoritması ve sonlu elemanlar yöntemi (SEY) tabanlı ANSYS-Maxwell yazılımı kullanılmıştır. Bu değerlere dayalı olarak motorun bilgisayar destekli tasarımı gerçekleştirilmiştir. Öncelikle motorun temel tasarım ve performans kriterleri belirlenmiştir. Motorun, tork dalgalanması, demir kaybı, verimliliği ve elektromanyetik analizi gibi parametreleri ANSYS-

[*] e-posta[1] : yildirim.ozupak@dicle.edu.tr ORCID ID: https://orcid.org/0000-0001-8461-8702 (Sorumlu Yazar)
e-posta[2] : mcinar@beu.edu.tr ORCID ID: https://orcid.org/0000-0002-1542-9120

Maxwell ile analiz edilmiş ve optimize edilmiştir. Ardından motorun elektriksel, manyetik ve performans analizleri yapılmıştır. Kullanılan yöntemler ile motor performansının nasıl değiştiği detaylı olarak incelenmiştir. Motor performans çalışmalarında çeşitli çalışma koşulları altında verim değerleri belirlenmiştir. ANSYS sonuçları ile PSO algoritması sonuçları karşılaştırılarak iyileştirme çalışmasının geçerliliği ve tasarım çalışmasının doğrulanması incelenmiştir. Analiz sonuçları, tasarlanan elektrik motorunun istenen güç değerlerini ve tasarım performans kriterlerini karşıladığını göstermiştir.

Anahtar Kelimeler: *KMSM, SEY, Verimlilik, Tasarım, PSO*

1. Introduction

Due to reasons such as decreasing oil resources, increasing oil prices, and an increase in environmental emission values, the tendency toward electric-driven vehicles has been increasing in recent years. It is a clear fact that important environmental problems have arisen as a result of the increasing use of fossil fuels with the development of industrialization and increased transportation. This negative environmental impact has led technology developments to more environmentalist approaches. Electric vehicle technology, which is probably the most prominent of these approaches, is entering daily life with an increasing speed [1-3]. A large number of electric passenger cars, electric bicycles and light electric vehicles are taking their place on the roads. For this purpose, vehicle manufacturers have introduced many electrically driven commercial vehicles to the market. These include vehicles such as the Toyota RAV4 EV, Chevrolet Volt, Tesla Model S and Renault Twizy. These trends bring along important developments in technologies related to electric vehicles. Today, most automotive manufacturers concentrate on research and development activities in the field of electric vehicles [4].

Many optimization problems arise when designing automobile engines [5-7]. Many involve multiple conflicting purposes. One of the most important stages in engine design is engine calibration [8-11], which is the adjustment or replacement of an internal combustion engine or control unit so that engine power achieves optimal fuel performance.

The engine control unit is one of the key parts in the engine that controls a series of actuators to achieve optimum performance. The control system reads values from a set of sensors and interprets the data using multidimensional performance maps to manipulate the motor actuators. An engine has a number of control systems, including air-fuel ratio control, idle speed control, engine start control, charge control, engine speed control, and fuel injection control. Optimizing engine control systems is an important task in the design of car engines.

Another research area in engine design is modeling of different parts of engines [12-14]. Modeling is done for different reasons. An example of this is the design and optimization of the controller system. Designing a controller using the real motor during the design process is an expensive and time-consuming action. For this reason, many researchers first build a model of the engine and then design, test and optimize their controllers on that model.

The efficiency of the electric motor, which is the key component of the electric drive system, is crucial because efficient energy use is required [15–17]. The objective of many academics and producers is to maximize the efficiency of electric motors while minimizing their losses [18]. Utilizing drive systems that consume the least amount of energy has two primary advantages: it extends the range of the vehicle and lowers the energy consumption per unit of distance per kilometer [19].

Many companies producing electric motors and automotive manufacturers that have started to produce electric vehicles are required to have high efficiency, high torque and low volume-weight characteristics. With the developments in magnetic materials and motor topologies, advances in electric motor designs continue rapidly [20-23].

Electric vehicles consist of four main subsystems. These are respectively battery and battery control system, electric propulsion system, electric motor driver and vehicle main control unit. The power required by the vehicle is supplied from the battery system. The battery control system constantly checks the temperature and charge status of the battery, depending on the power needs of varying duration and value, and transmits information to the vehicle main control unit. An electric motor is used in the vehicle propulsion system. Various types of motors such as permanent magnet synchronous motor, squirrel cage PMS motor and switched reluctance motor, AS-PMSM can be used in electric vehicles. Efficiency in PMSM motors also depends on many interrelated parameters. A four-zone driver is used to provide variable frequency torque control of the selected motor.

In this study, the design and analysis of AS-PMSM at 110 kW at maximum operation for an electric vehicle propulsion system is demonstrated. The results are achieved by running the design equations of PMSM and specific parameters into MATLAB Simulation, which is performed by the PSO. The engine created to examine the findings is assessed with FEM-based software (ANSYS Electronics Desktop). As a result of the analyzes carried out, it has been seen that the designed electric motor provides the targeted performance values depending on the design constraints.

2. Material and Method

2.1. Design of PMSM

Since most of the PMS motors used in the industry are operated without a driver, they are designed for a fixed operating voltage and frequency depending on the mains voltage and frequency. These data assist the designer in the selection of relevant design parameters such as number of poles, number of slots, slot type, air gap, current and flux densities during design. However, as in electric vehicles, PMS motors working with driver work at variable frequency, voltage and power values. Due to this, the majority of the information supplied, including the stator-rotor groove combination chosen for PMS motors produced for fixed operating points, is no longer applicable. In Figure 1, the speed-dependent torque and power characteristics of the electric motors working with the driver used in electric vehicles are shown [17].

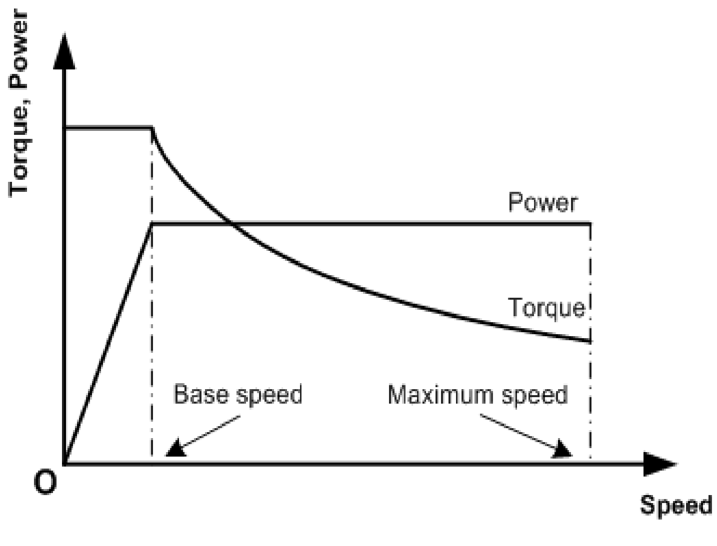

Figure 1. Speed-dependent torque and power characteristics of driver-operated electric motors in electric vehicles

In the PMSM design to be used for the electric vehicle, first of all, the fundamental frequency value, from which the nominal power value is desired, must be determined. The point to be considered here is that the motor operating frequency range does not reach high values when determining the number of poles. This causes an increase in the frequency-dependent losses in the motor design. In addition, the maximum operating speed of the motor is directly related to the overturning torque. It is desired that the engine overturning torque be high in order to offer the appropriate maximum working speed. Leakage inductances are attempted to be reduced as much as feasible in the design in order to accomplish this. Second, the design takes into account the lowest and highest voltage values that the electric car battery can provide.

2.2. Mathematical Model

The voltage equations in the d-q reference plane of the motor examined by FEM are different from the voltage equations designed for the general equivalent circuit.

$$\lambda = \int_1 \emptyset dl \tag{1}$$

where, λ flux, ∅ vector potential and l is the length of the line line. The Fourier expansion of the magnet flux used in the motor is given in equation (2).

$$\lambda_m = \sum_{n=1}^{\infty} \lambda_{m(2n-1)} \sin((2n-1)\theta_r) \tag{2}$$

It is considered sufficient to use harmonic coefficients up to the 7th harmonic in the modeling of magnet fluxes.

$$\lambda_m = \lambda_{m1} sin\theta_r + \lambda_{m3} sin3\theta_r + \lambda_{m5} sin5\theta_r + \lambda_{m7} sin7\theta_r \tag{3}$$

If equation 4, which is given as the Park transformation equation, is applied to equation 3, the expression of the fluxes passed by the magnets through the stator windings in the rotor reference plane is given in equation 5.

$$\begin{bmatrix} f_q \\ f_d \\ f_0 \end{bmatrix} = \frac{2}{3} \begin{bmatrix} \cos(\theta_r) & \cos\left(\theta_r - \frac{2\pi}{3}\right) & \cos\left(\theta_r + \frac{2\pi}{3}\right) \\ \sin(\theta_r) & \sin\left(\theta_r - \frac{2\pi}{3}\right) & \sin\left(\theta_r + \frac{2\pi}{3}\right) \\ \frac{1}{2} & \frac{1}{2} & \frac{1}{2} \end{bmatrix} \begin{bmatrix} f_a \\ f_b \\ f_c \end{bmatrix} \tag{4}$$

Here *f* represents one of the motor current, voltage and flux variables. Motor magnets are modeled by equation 5 and equation 6.

$$\lambda_{mq} = \lambda_{m5} \sin(6\theta_r) + \lambda_{m7} \sin(6\theta_r) \tag{5}$$

$$\lambda_{md} = \lambda_{m1} - \lambda_{m5} \cos(6\theta_r) + \lambda_{m7} \cos(6\theta_r) \tag{6}$$

The total flux values passing through the windings of the motor are given in equation 7 and equation 8.

$$\lambda_q = L_q i_q + \lambda_{mq} \tag{7}$$

$$\lambda_d = L_d i_d + \lambda_{md} \tag{8}$$

The simplified d-q equivalent circuit of the motor model obtained by FEM is given in Figure 2.

In Figure 2, $v_{q\lambda}$ ve $v_{d\lambda}$ are voltages resulting from flux changes and are given in equation 9 and equation 10.

$$v_{q\lambda} = w_r(L_d i_d + \lambda_{m1} + 5\lambda_{m5} \cos(6\theta_r) + 7\lambda_{m7} \cos(6\theta_r)) \tag{9}$$

$$v_{d\lambda} = w_r(L_q i_q - 5\lambda_{m5} \sin(6\theta_r) + 7\lambda_{m7} \sin(6\theta_r)) \tag{10}$$

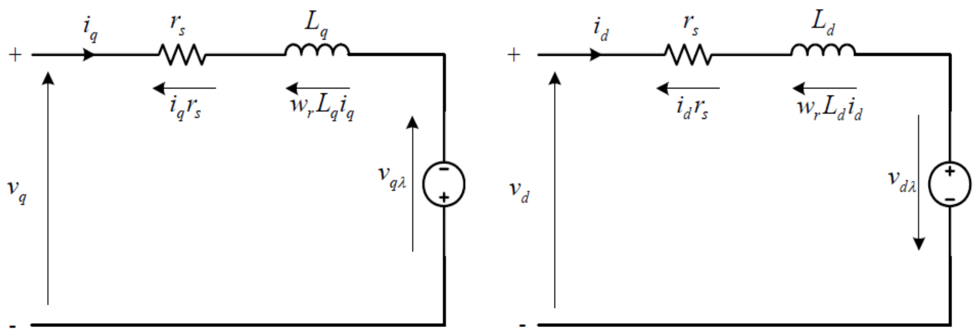

Figure 2. Simplified d-q equivalent circuit of the motor model obtained by FEM.

The voltage equations of the motor are presented in equation 11 and equation 12.

$$v_{q\lambda} = r_s i_q + L_q p i_q + w_r(L_d i_d + \lambda_{m1} + 5\lambda_{m5}\cos(6\theta_r) + 7\lambda_{m7}\cos(6\theta_r)) \tag{11}$$

$$v_{d\lambda} = r_s i_d + L_d p i_d - w_r(L_q i_q - 5\lambda_{m5}\sin(6\theta_r) + 7\lambda_{m7}\sin(6\theta_r)) \tag{12}$$

The electrical moment expression is given in equation 13.

$$T_e = \frac{3P}{2}\left[(\lambda_{m1} + 5\lambda_{m5}\cos(6\theta_r) + 7\lambda_{m7}\cos(6\theta_r)\, i_q - 5\lambda_{m5}\sin(6\theta_r) - 7\lambda_{m7}\sin(6\theta_r)\right] i_q \tag{13}$$

2.3. Design Parameters

The electric drive motor is one of the subsystems of the electric vehicle such as battery, driver, control unit and battery control system. For this reason, there are also constraints related to other subsystems in engine design. Data affecting engine design depending on other subsystems are given in Table 1.

Table 1. Basic parameters of the motor

Name	**Value**
"Operation Type"	Motor
"Load Type"	"Const Power"
"Rated Output Power"	85.98 kW
Maximum power	110kW
"Rated Voltage"	220 V
"Maximum Speed"	13300 rpm
Tork	185 Nm
Efficiency	96.2 %
"Operating Temperature"	75 cel

Before starting the motor design, in addition to the performance values specified in Table 1, electrical and magnetic parameters should also be determined. These values used in the design are given in Table 2.

The nominal voltage value used in the design was chosen as 220 V, which is the lowest voltage value of the battery. Thus, the motor is designed to provide the desired torque value even at the lowest battery voltage. The electrical design of the motor was balanced between nominal and maximum power values, and parameters that directly impact the thermal performance of the motor, such as current density, were not selected too closely to the maximum permitted values for nominal operation. Thus, it is aimed to ensure that the maximum power that can be drawn from the engine is as long as possible.

Table 2. Electrical and magnetic parameters of the motor

Name	Value
Stator-Teath Flux Density	0.78 T
Stator-Yoke Flux Density	0.79 T
Rotor-Yoke Flux Density	0.43 T
Air-Gap Flux Density	0.63 T
Magnet Flux Density	0.98 T
Stator Teath Ampere Turn	2.4 A.T
Stator Yoke Ampere Turn	2.7 A.T
Rotor Yoke Ampere Turn	0.96 A.T

The dimensions of the motor were determined depending on the values specified in Table 1 and Table 2. While determining the dimensions of the motor, the output coefficient method was used [18,19]. Depending on the predetermined design values, the dimensioning of the motor, stator and rotor design were carried out. The thickness of the lamination material to be used is 0.3 mm, the magnetic saturation value is 2.4 T and the iron loss is 1.043 kW. Depending on the analytical and magnetic analysis results, improvements were made in the design. ANSYS RMxprt and Maxwell-2D computer packages were used for analytical and magnetic design. The lamination geometry of the designed electric motor and the parameters related to the geometry are presented in Figure 3 and Table 3, respectively.

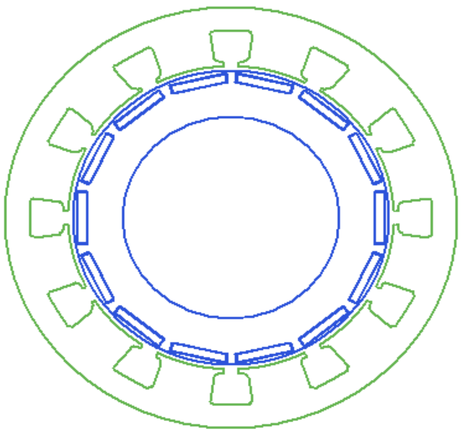

Figure 3. Stator and rotor geometry

Table 3. Mechanical design parameters of the motor

Name	Value
Outer diameter of the stator core	300mm
Inner diameter of the stator core	217mm
Length of the stator core	75mm
Stacking Factor	0.95
Steel type of the stator core	M27_29G
Outer diameter of the rotor core	210mm
Inner diameter of the rotor core	145mm
Length of the rotor core	75mm
Steel type of the rotor core	M27_29G

3. Result and Discussion

3.1. Analysis of PMSM with Particle Swarm Optimization Algorithm

Particle Swarm Optimization (PSO) was developed in 1995 by J. Kennedy and R. C. Eberhart [24]. It is a heuristic algorithm inspired by the behavior of bird flocks. When looking for food, birds follow the bird (leader) that is thought to be closest to the food. The leader may change during the search for food. The new bird leader that sees the food is selected and all the birds in the flock continue their search for food by turning to the new leader. They communicate among themselves to determine the leader. Each bird in the flock is called a particle and represents a solution. The current position of each bird is an entry for the function whose solution is sought. Therefore, while the bird moves, it transmits each position to the function and a solution is produced for the current position. The obtained solution is evaluated and the fitness value of that solution is obtained. The fitness value is a measure of whether the result has been achieved or not. If a suitable result is found in line with the criteria, the search ends. If no suitable result is found, the birds continue to wander in the search space. A general block diagram of the PSO is given in Figure 4 [25]. Before the algorithm starts to run, a crowd is created and initial values such as speed and position are assigned. The most important feature that distinguishes PSO from classical optimization algorithms is that it has a simpler structure because the number of parameters to be adjusted is low and it does not need derivative information.

In Particle Swarm Optimization, a randomly determined set of possible solutions is first generated. Each row of the solution set created here constitutes a particle, and each column constitutes the swarm. The matrix created here is actually randomly determined values of Kp, Ki and Kd [26].

Each element of this matrix is applied to the system to be optimized and pbest, which is the best of the applied particles, and gbest, which is the best of the swarm, are calculated. In the first iteration, the pbest of each particle is equal to itself. The particle corresponding to the best value obtained from here is chosen as gbest. After these two best values are found; The particle, its velocity and position are updated according to equations (14) and (15) below, respectively. After calculating the new position values, these values are used to return to the beginning of the iteration, and the fitness values are calculated and the pbest and gbest values are updated. The proceedings are continued until the termination condition is met [26].

$$v_i^{k+1} = v_i^k + c_1 * rand_1^k * (pbest_i^k - X_i^k) + c_2 * rand_2^k * (gbest^k - X_i^k \tag{14}$$

$$X_i^{k+1} = X_i^k + V_i^{k+1} \tag{15}$$

Where, a randomly generated number between rand (0-1), i represents the particle number, and k represents the number of iterations. c_1 and c_2 are learning factors. These are constants that orient particles towards the pbest and gbest positions. c1 directs the movement according to the experience of the particle itself, and c_2 according to the experiences of other particles in the swarm. Choosing lower values allows particles to circulate far from the target area before being drawn towards it. However, it may take longer to reach the target. On the other hand, choosing high values may cause unexpected movements to occur and the target area to be bypassed, while accelerating reaching the target.

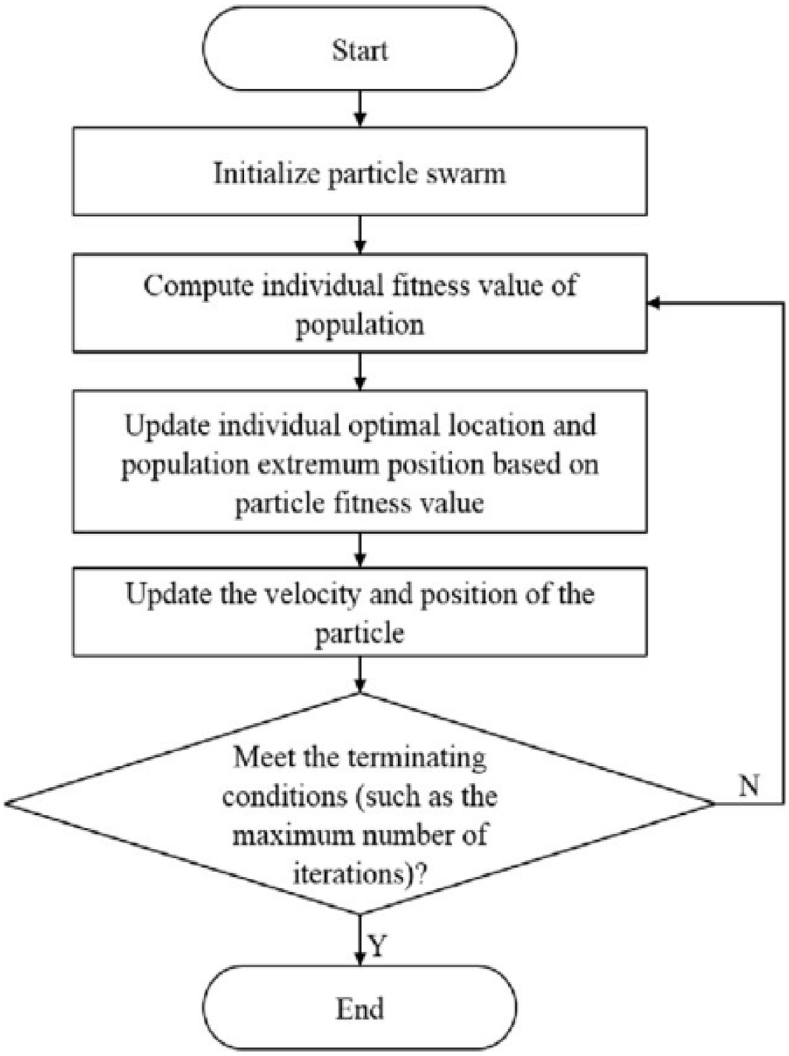

Figure 4. Flowchart of the PSO algorithm

The optimum parameter values for the particle swarm optimization algorithm in the developed Matlab program are given in Table 4. The optimum engine values were obtained by running the program 30 times.

Table 4. Parameters and values used in the particle swarm optimization algorithm

Parameter	**Value**
Population size	100
Maximum iteration	100
Number of runs	30
Cognitive constant	2
Social constant	2
Max inertia weight	0,9
Min inertia weight	0,4

Figure 5 displays the efficiency of the electric motor created using these parameters, along with iron and copper losses.

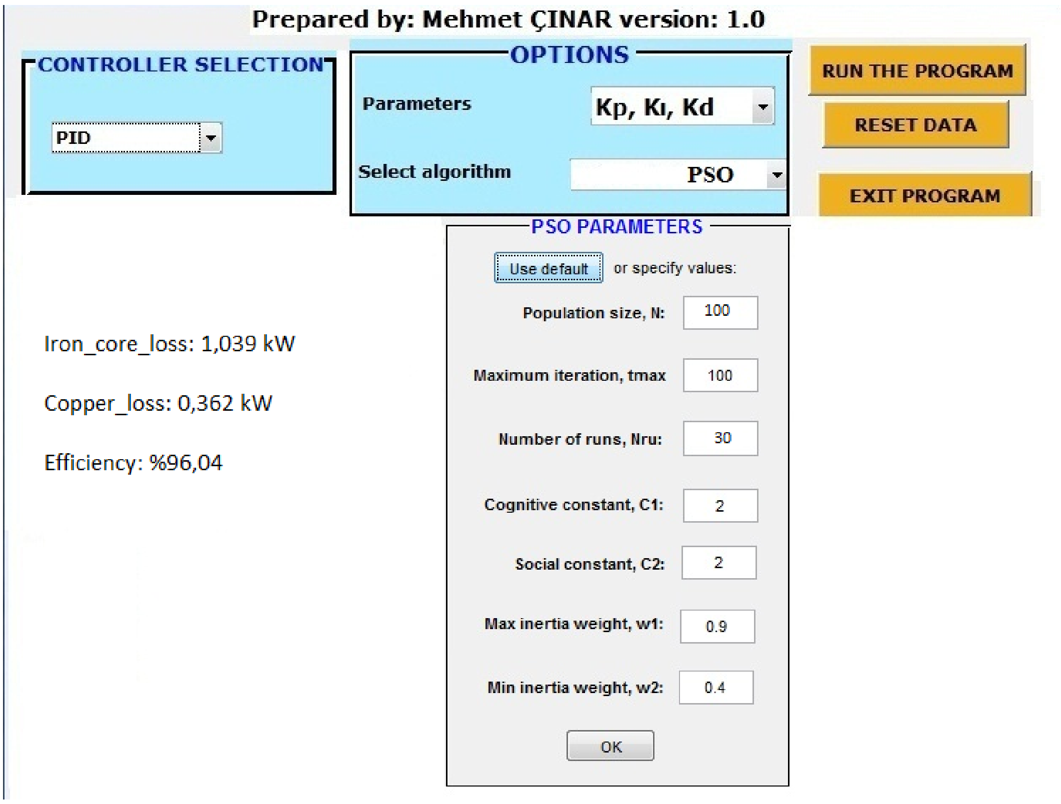

Figure 5. Motor parameter values were obtained with the help of the developed program

3.2. ANSYS Analysis Results

According to the structural parameters given in the previous section, the Finite Element Model of the engine was created and electromagnetic field finite element analysis was performed on the first structural design results and the simulation parameters of the first design results were obtained. In Figure 6, the swing torque is given when the motor is running at no load. It can be seen from the figure that this torque is small and has a peak-to-peak value of 0.35 Nm.

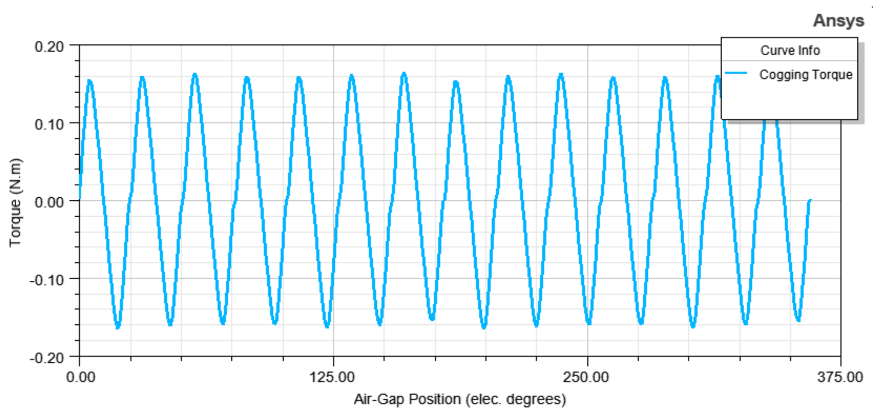

Figure 6. Torque curve in gears

The air gap-flux density value of the motor is given in Figure 7. In Figure 8, the curve of the torque ripple is presented. The torque ripple here is due to the instantaneous values of the current.

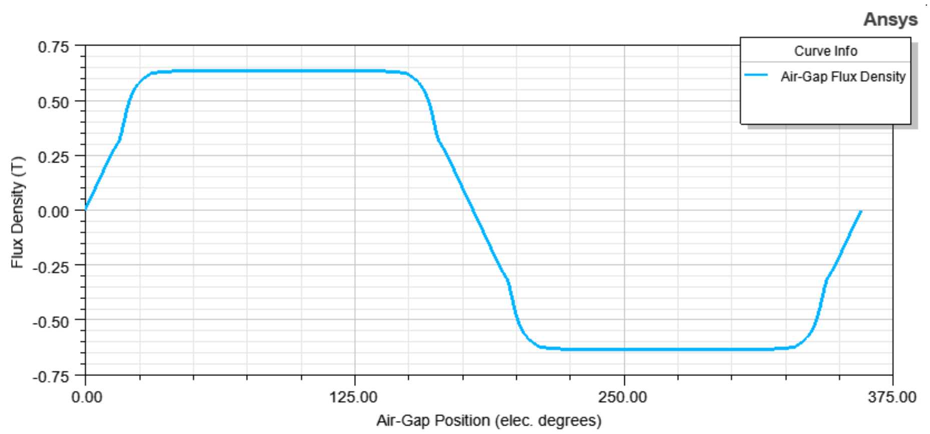

Figure 7. Air gap-flux density plot

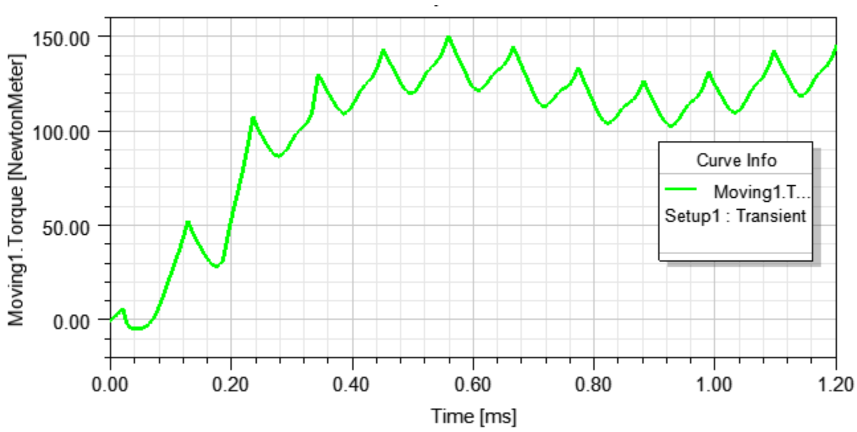

Figure 8. Torque curve at rated operating condition

As can be seen, the torque value reaches the desired nominal torque value in the nominal operating condition. The vibration value on the torque chart is within acceptable limits. The distribution of flux lines obtained when the analytically calculated currents shown in Figure 9 are applied to the motor windings for the nominal operating condition are shown in Figure 10.

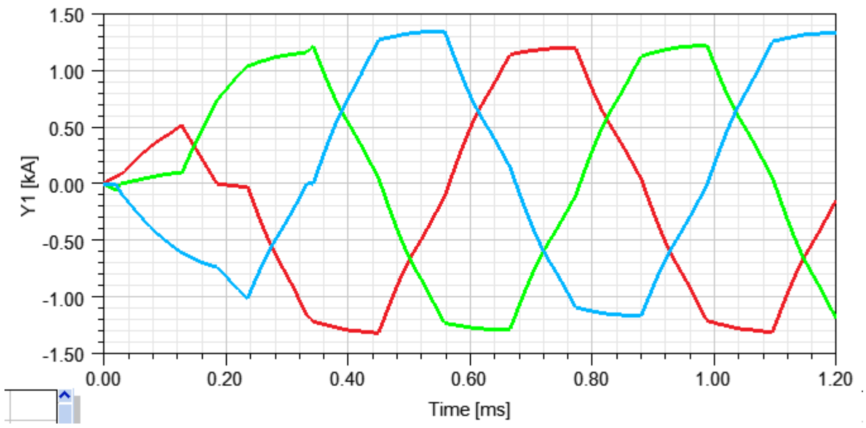

Figure 9. Winding currents at rated operating condition

The maximum inrush current value can be up to 1.2 kA. This current value is not a continuous operating current. Litz conductor is used. The conductor cross section is determined in the ANSYS program depending on the electrical values of the motor.

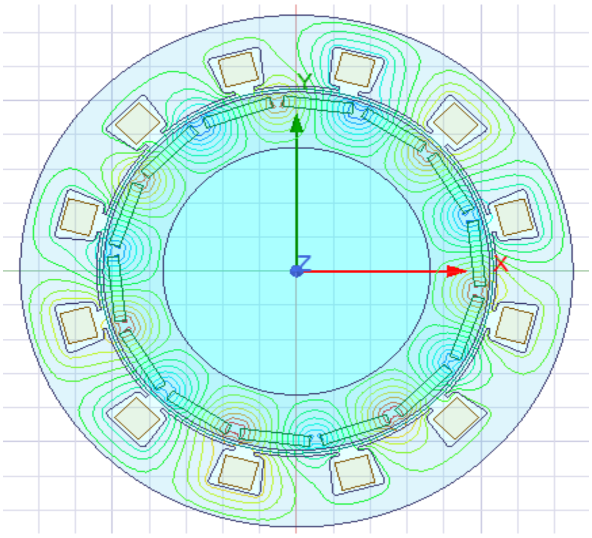

Figure 10. Distribution of flux lines at nominal operating condition

As can be seen, the flux lines are evenly distributed and the desired winding poles are formed. The magnetic flux density distribution in the motor core in the rated operating condition is given in Figure 11.

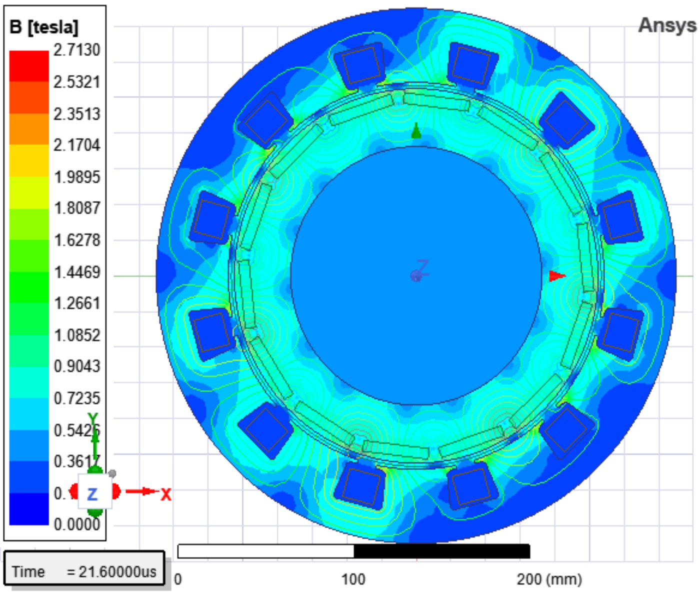

Figure 11. Flux density distribution at rated operating condition

As can be seen, flux densities in general do not exceed 2T. Although there are occasional overhangs in narrow areas such as the openings of the gutters, these are below the magnetic saturation value of the material used, which is 2.3T. The efficiency-torque curve obtained in the nominal operating condition is presented in Figure 12.

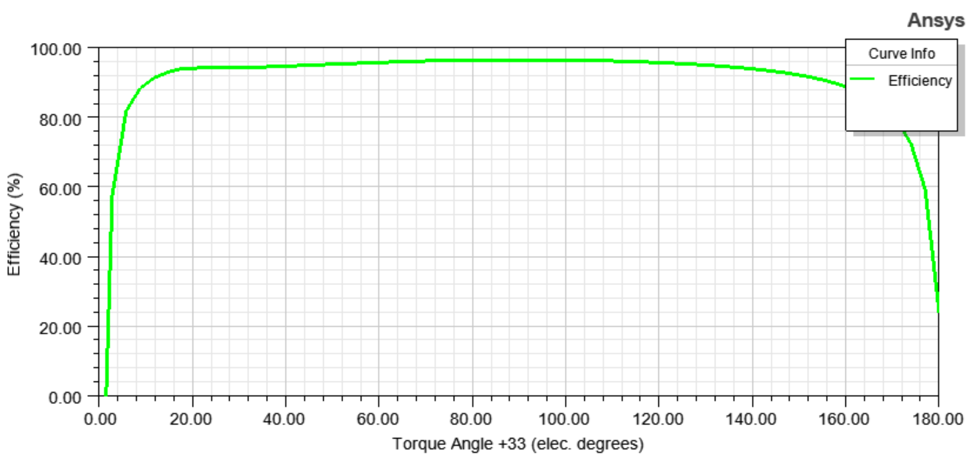

Figure 12. Efficiency of the engine

Finally, the general analysis results for the motor design for rated operation are given in Table 5.

Table 5. Analysis results of PMSM performed with ANSYS-Maxwell and MATLAB-PSO

Parameter	**ANSYS-Value**	**MATLAB-PSO**
Input power	89.6 kW	89.6 kW
Rated Moment	186.7 Nm	185.4 Nm
Electrical output power	85.98 kW	86,05 kW
Iron-core loss	1.043 kW	1.039 kW
Copper loss	0.35 kW	0.362 kW
Efficiency	96.2 %	96.04 %
Rated speed	5840 rpm	5819
Maximum speed	13300 rpm	13300

As seen in Table 5, the targeted power, torque and efficiency values were obtained. For a nominal input voltage of 220 V and a nominal power of 85.98 kW, the overturning torque and maximum operating speed of the motor meet the desired design values. In addition, current densities are below the values specified in the design criteria. Thus, the designed motor meets all the desired design criteria electrically and magnetically. Current densities are lower than the maximum allowable values in the design. The reason for this is that a balanced design is desired considering the maximum power requirement. Forcing the design limit values for the nominal operating condition shortens the maximum power draw time from the motor, depending on the current density value that will increase in case of maximum power demand.

3.3. Investigation of Motor Performance Based on Voltage, Frequency and Power Variation

In electric vehicle applications, the frequency and torque value of the engine are constantly changing, depending on the instantaneous driving performance parameters. In addition to these variables, the voltage that the battery module can provide in the vehicle decreases gradually depending on the power consumption. While performing the motor design, it is desired that the motor data remain within the specified design constraints at different operating points depending on these three basic variables. In Table 6, the performance values obtained when the voltage and output power change from the nominal value to their maximum values are given.

Table 6. Motor ratings at nominal and maximum power operating conditions

V_s (V)	P_0 (kW)	B_t (T)	Efficiency (%) (ANSY)	Efficiency (%) (PSO)
220	85.98	1.84	96.28	96.04
220	110	1.82	95.49	95.1
250	85.98	2.13	95.98	95.52
250	110	2.09	95.71	95.34

V_s given in the table shows the input voltage, P_0 shows the output power, B_t shows the flux density in the teeth. As can be seen, if the input voltage and the desired output power requirement change from their nominal values to their maximum values, both electrical and magnetic values of the designed motor remain within the design limits. This shows that a balanced engine design has been carried out. Thus, when needed, maximum power from the engine will be provided for a longer period of time without forcing the engine. This helps in improving the thermal performance of the motor.

4. Conclusion

In this study, PMSM design and analysis results to be used in electric vehicle propulsion systems are presented. First of all, the performance parameters of the engine and the values related to other subsystems such as the battery were determined and the design of the engine was carried out considering these. As a result of the computer aided analytical and magnetic analyzes carried out, it has been seen that the designed engine provides the desired performance values in the nominal operating condition in accordance with the determined criteria. The performance of the motor is also investigated depending on the changing voltage, power and frequency values. When the engine parameters obtained in Figure 5 with the help of the particle swarm optimization algorithm are examined, the efficiency of the engine is calculated as 96.04%. In addition, it is seen that the other calculated motor parameters are close to the values calculated as a result of the ANSYS program. With these analyzes, it has been observed that a balanced design has been carried out to preserve the performance of the motor depending on these changes, and the motor data does not exceed the specified electrical and magnetic design limits.

Acknowledgment

This study; It was supported by Dicle University Scientific Research Project unit within the scope of the project numbered SİLVAN-MYO.22.001.

References

[1] Lee J.H., Kim D., Song J., Jung S., Kim Y., (2016) Design of 100kW Propulsion Motor for Electric Conversion Vehicle Based on Vehicle Driving Performance Simulation, IEEE Transportation Electrification Conference and Expo, Busan-Korea (South), 412-416, 1-4.

[2] Bouscayrol A., Boulon L., Hofman T., Chan C.C., (2016) Special Section on Advanced Powertrains for More Electric Vehicles, IEEE Transactions on Vehicular Technology, 6 (3), 995 – 997.

[3] Zhu S., Hu Y., Liu C., Wang K., (2018) Iron Loss and Efficiency Analysis of Interior PM Machines for Electric Vehicle Applications, IEEE Transactions on Industrial Electronics, 65 (1), 114-124.
[4] Özüpak Y. (2022) Efficiency Analysis of BLDC for variable magnetic field. 2022. MANAS Journal of Engineering, Volume 10 (Issue 1).
[5] A. Belmondo, F. Giuggioli, and B. Giorgi, (1983) Optimization of ferrographic oil analysis for diesel engine wear monitoring," Wear, vol. 90, no. 1, pp. 49 – 61.
[6] J. J. Kim and H. Y. Kim, (1997) Shape design of an engine mount by a method of parameter optimization," Computers & Structures, vol. 65, no. 5, pp. 725 – 731.
[7] C. Gagne, M. Gravel, and W. L. Price, (2006) Solving real car sequencing problems with ant colony optimization," European Journal of Operational Research, vol. 174, no. 3, pp. 1427 – 1448, 2006.
[8] D. Lowe and K. Zapart, (1997) Validation of neural networks in automotive engine calibration," in fifth International Conference on Artificial Neural Networks (Conf. Publ. No. 440), pp. 221–226.
[9] K. Zeng, S. Lv, B. Liu, F. Ma, and Z. Huang, (2006) Development and calibration on an electronic control system of cng engine," in IEEE International Conference on Vehicular Electronics and Safety. ICVES, pp. 204–208.
[10] C. Vong, P. Wong, and H. Huang, (2009) Case-based reasoning for automotive engine electronic control unit calibration," in Information and Automation, 2009. ICIA '09. International Conference on, pp. 1380–1385.
[11] A. Rosato and S. Sibilio, (2012) Calibration and validation of a model for simulating thermal and electric performance of an internal combustion engine-based micro-cogeneration device," Applied Thermal Engineering, vol. 45-46, pp. 79 – 98.
[12] L. Brzozowska, K. Brzozowski, and J. Nowakowski, (2005) An application of artificial neural network to diesel engine modelling," in Intelligent Data Acquisition and Advanced Computing Systems: Technology and Applications. IDAACS 2005. IEEE, 2005, pp. 142–146.
[13] K. Atashkari, N. Nariman-Zadeh, M. Golcu, A. Khalkhali, and A. Jamali, (2007) Modelling and multi-objective optimization of a variable valvetiming spark-ignition engine using polynomial neural networks and evolutionary algorithms," Energy Conversion and Management, vol. 48,no. 3, pp. 1029 – 1041.
[14] C. Hametner and S. Jakubek, (2011) Combustion engine modelling using an evolving local model network," in Fuzzy Systems (FUZZ), IEEE International Conference on, 2011, pp. 2802–2807.
[15] Liu J., Gong C., Wu Z., (2017) Influence Research of Rotor Structure Parameters on the Performance of IPMSM, 20th International Conference on Electrical Machines and Systems (ICEMS), Sydney-Australia, 1-5, 11-14.
[16] Rakesh K., Sanjeevikumar P., (2019) Electric Vehicles for India: Overview and Challenges , IEEE India Info. Vol. 14 No. 2.
[17] Bozhidar S., George T., Plamen R., Gerasimos P., Leonidas D., (2017) Finite element analysis of rotating electrical machines- an educational approach‖, IEEE Global Engineering Education Conference (EDUCON).
[18] Chan-B. P., Geochul J., (2017) Design and Analysis of Magnetic-Geared Permanent Magnet Synchronous Motor for Driving Electric Vehicles‖, IEEE - International Conference on Electrical Machines and Systems (ICEMS).
[19] Emma A., G., Torbjörn T., (2016) Performance Analysis of Current BEVs Based on a Comprehensive Review of Specifications‖, IEEE transactions on transportation electrification, vol. 2, no. 3.
[20] Yamano, K., Morimoto, S., Sanada, M., Inoue Y., (2016) Basic Study on Design of Surface Permanent Magnet Synchronous Motor Using Design Assist System of PMSM‖, IEEE - International Conference on Electrical Machines and Systems (ICEMS).
[21] Yamazaki K, Kumagai M, Ikemi T and Ohki S., (2013) IEEE Transactions on Industry Applications vol 49 pp 2478–86
[22] Özüpak, Y., (2022) Investigation of the Effect of Design Parameters of Small Brushless DC Motors on Motor Performance by Finite Element Method, Brilliant Engineering, 3, 4658. https://doi.org/10.36937/ben.2022. 4658.

[23] Claudio B, Fabio I, Emilio L, Alberto B and Matteo D (2012) IEEE Transactions on Magnetics vol 48 pp 2685-93
[24] Federico Marini, Beata Walczak, (2015) Particle swarm optimization (PSO). A tutorial, Chemometrics and Intelligent Laboratory Systems, Volume 149, Part B, Pages 153-165, ISSN 0169-7439, https://doi.org/10.1016/j.chemolab.2015.08.020.
[25] M. Reyes-Sierra and C. A. C. Coello, (2006) Multi-Objective Particle Swarm Optimizers: A Survey of the State-of-the-Art," International Journal of Computational Intelligence Research, Vol. 2, No. 3, 2006, pp. 287-308.
[26] T. M. Shami, A. A. El-Saleh, M. Alswaitti, Q. Al-Tashi, M. A. Summakieh and S. Mirjalili, (2002) Particle Swarm Optimization: A Comprehensive Survey, in *IEEE Access*, vol. 10, pp. 10031-10061, 2022, doi: 10.1109/ACCESS.2022.3142859